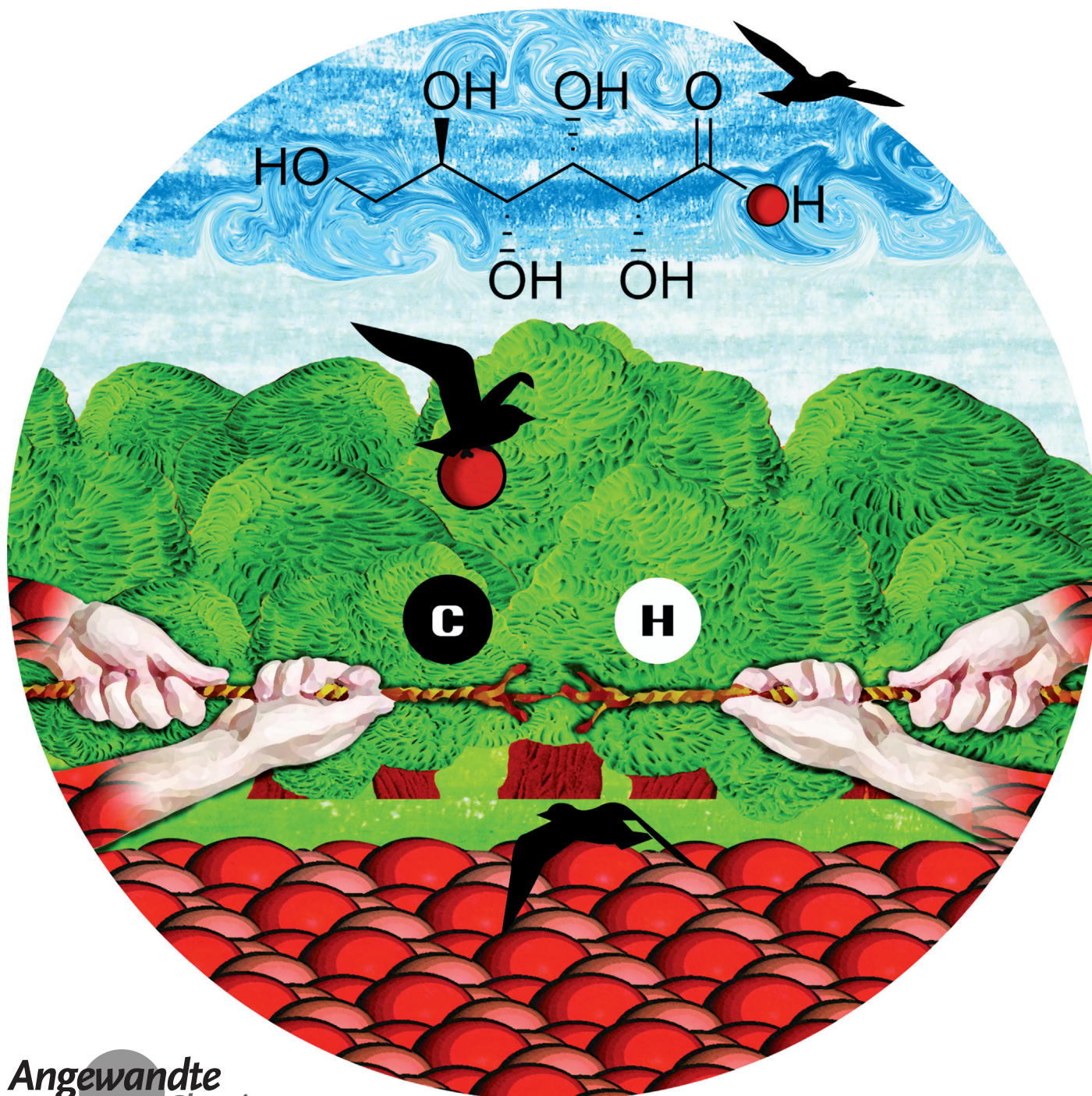


# Biomass Oxidation: Formyl C–H Bond Activation by the Surface Lattice Oxygen of Regenerative CuO Nanoleaves\*\*

Prince N. Amaniampong, Quang Thang Trinh, Bo Wang, Armando Borgna, Yanhui Yang,\* and Samir H. Mushrif\*



**Abstract:** An integrated experimental and computational investigation reveals that surface lattice oxygen of copper oxide (CuO) nanoleaves activates the formyl C–H bond in glucose and incorporates itself into the glucose molecule to oxidize it to gluconic acid. The reduced CuO catalyst regains its structure, morphology, and activity upon reoxidation. The activity of lattice oxygen is shown to be superior to that of the chemisorbed oxygen on the metal surface and the hydrogen abstraction ability of the catalyst is correlated with the adsorption energy. Based on the present investigation, it is suggested that surface lattice oxygen is critical for the oxidation of glucose to gluconic acid, without further breaking down the glucose molecule into smaller fragments, because of C–C cleavage. Using CuO nanoleaves as catalyst, an excellent yield of gluconic acid is also obtained for the direct oxidation of cellobiose and polymeric cellulose, as biomass substrates.

**M**etal oxides are well-known oxidation catalysts.<sup>[1]</sup> Oxidation of hydrocarbons on metal oxides is believed to occur by a Mars-van-Krevelen-type mechanism, using the lattice oxygen.<sup>[2]</sup> However, surface-adsorbed oxygen is also reported to participate in the reaction.<sup>[2a,f,3]</sup> It is proposed that surface oxygen leads to “electrophilic oxidation”; whereas the lattice oxygen leads to “nucleophilic oxidation” of the hydrocarbons.<sup>[2a,d]</sup> The nature and role of these different oxygen species and the underlying bond activation mechanism<sup>[4]</sup> are not yet fully understood. Similarly, in the case of molecules with oxygen-containing functional groups, exchange of surface lattice oxygen with the reactant is reported,<sup>[1c,5]</sup> with little insight into

the role of lattice oxygen in catalyzing the oxidation reaction. In alignment with the extensive recent research in converting lignocellulosic biomass to fuels and chemicals, significant interest is now generated in oxidizing cellulosic sugars into sugar acids and its derivatives,<sup>[6]</sup> using metal oxides as catalysts.<sup>[7]</sup>

Hence, herein 1) we perform the oxidation of glucose, cellobiose and cellulose on a CuO catalyst, in the form of nanoleaves, with an excellent yield of gluconic acid, 2) using scanning electron microscopy (SEM), high-resolution transmission electron microscopy (HRTEM), X-ray diffraction (XRD), and isotope labeling experiments we demonstrate that the lattice oxygen in the catalyst is consumed in the reaction and that the catalyst regains its (chemical) structure, morphology, and activity upon oxygen treatment, and 3) using DFT calculations we reveal the role of surface lattice oxygen in activating the formyl C–H bond in sugars. The complete reaction mechanism, involving the insertion of the surface lattice oxygen into the sugar molecule, in perfect agreement with the experimental findings, is revealed. The C–H bond

**Table 1:** Reactant conversion and gluconic acid yields for the CuO-catalyzed oxidation of glucose, cellobiose, and cellulose. Reaction temperature = 150 °C. The optimum glucose/catalyst ratio of 1:1 is used (refer to Table S1 in the Supporting Information for details).

Biomass Substrate	Catalyst <sup>c</sup>	Reaction time [min]	Conversion [%]	Gluconic acid yield [%]
glucose <sup>[a]</sup>	CuO fresh	30	100	86.8 ± 1.4
glucose	CuO spent	30	100	2.0 ± 1.8
glucose <sup>[a]</sup>	CuO regenerated	30	100	85.4 ± 0.8
cellobiose <sup>[a,b]</sup>	CuO fresh	30	98.5	65.7 ± 0.5
cellobiose <sup>[a,b]</sup>	CuO regenerated	30	100	71.7 ± 1.1
cellulose <sup>[a,b]</sup>	CuO fresh	180	96.8	59.0 ± 2.5

[a] Reactor purged with nitrogen. [b] Reaction temperature = 200 °C. [c] The fresh catalyst refers to the as-synthesized catalyst, spent catalyst refers to the catalyst which has undergone one reaction cycle, and regenerated catalyst refers to the catalyst which, after one reaction cycle, is reoxidized for 120 minutes under oxygen flow.

[\*] P. N. Amaniampong,<sup>[†]</sup> Dr. Q. T. Trinh,<sup>[†]</sup> Prof. Y. Yang, Prof. S. H. Mushrif

School of Chemical and Biomedical Engineering  
Nanyang Technological University  
62 Nanyang Drive, Singapore 637459 (Singapore)  
E-mail: YHYang@ntu.edu.sg  
SHMushrif@ntu.edu.sg

P. N. Amaniampong,<sup>[†]</sup> Dr. B. Wang, Dr. A. Borgna  
Institute of Chemical and Engineering Sciences  
A\*STAR (Agency for Science, Technology and Research)  
1 Pesek Road, Jurong Island, Singapore, 627833 (Singapore)

[†] These authors contributed equally to this work.

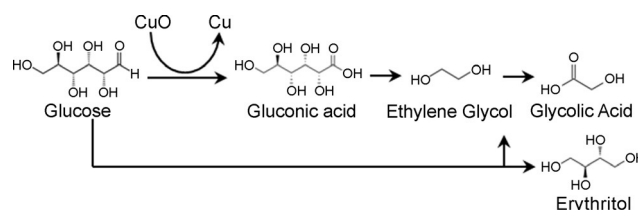
[\*\*] Financial support from the Singapore Agency for Science, Technology and Research, A\*STAR (P.N.A., B.W., and A.B.), Nanyang Technological University Singapore (S.H.M. and Q.T.T.), the National Research Foundation (NRF), Prime Minister's Office, Singapore under its Campus for Research Excellence and Technological Enterprise (CREATE) program and AcRF Tier 1 (grant number RG129/14), MOE, Singapore (Y.Y.) is acknowledged. We thank Prof. Xu Rong and Mrs. Christine Veras for their help in isotope-labeling experiments and in the design of the frontispiece art, respectively.



Supporting information for this article is available on the WWW under <http://dx.doi.org/10.1002/anie.201503916>.

activation by surface lattice oxygen is compared with that of chemisorbed oxygen on the surface. The crucial role of surface lattice oxygen in the oxidation of glucose to gluconic acid, with minimum C–C cleavage, is explained.

The conversions of the oxidation of glucose, cellobiose, and cellulose on CuO nanoleaves and the yields of gluconic acid are shown in Table 1. The simplified reaction scheme for glucose oxidation on CuO is shown in Scheme 1. The fresh catalyst gives more than 85% yield of gluconic acid from glucose; whereas, the spent catalyst results in the formation of only smaller polyols like ethylene glycol, erythritol, and



**Scheme 1.** Simplified reaction scheme for the oxidation of glucose catalyzed by CuO.



smaller acids like glycolic, lactic, and formic acids. However, after the oxidative regeneration, the catalyst regains its selectivity towards gluconic acid. The conversion of glucose and the yield of gluconic acid did not change significantly, irrespective of the reactor being purged by nitrogen or not. This suggests that dissolved oxygen does not play any role in the reaction and that CuO is the source of oxygen in the oxidation reaction. At reaction temperatures higher than 150 °C, gluconic acid yield decreases and the yield of C<sub>1</sub>–C<sub>4</sub> acids increases, suggesting the cleavage of C–C bonds. The CuO catalyst also gives excellent yield of gluconic acid, with cellobiose and cellulose as biomass substrates. However, higher temperatures are required for cellobiose and cellulose, since H<sub>3</sub>O<sup>+</sup> ions, which are reversibly generated in hot water at higher temperatures,<sup>[8]</sup> catalyze the hydrolysis of cellobiose and cellulose to glucose.

The XRD pattern of as-synthesized CuO nanoleaves (compare Figure 1a) shows signature peaks of copper(II) oxide, dominated by CuO(111) and CuO(–111) surfaces ( $2\theta = 38.6$  and  $35.5^\circ$ , respectively).<sup>[9]</sup> Additionally, a control

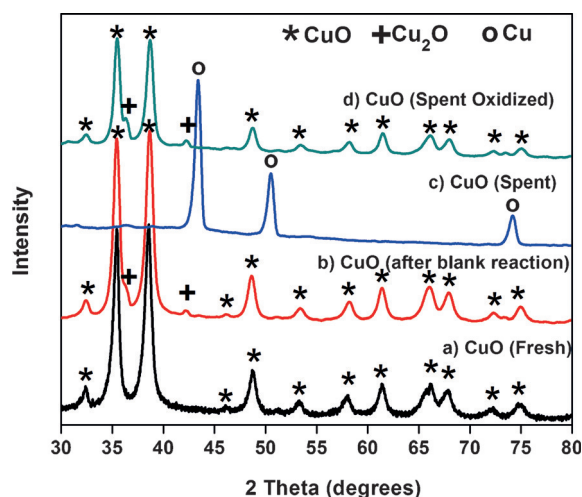


**Figure 1.** X-ray diffractograms of CuO nanoleaves samples. a) Fresh catalyst sample. b) Catalyst sample under reaction conditions, but without any reaction. c) Spent catalyst after the glucose oxidation reaction. d) Regenerated/reoxidized catalyst.

experiment (denoted as blank reaction in Figure 1b) was performed where the catalyst and deionized water, without the addition of any biomass substrate, were stirred in the batch reactor at 473 K for 30 minutes. The XRD pattern of the dried catalyst is identical to that of the fresh catalyst, strongly suggesting that the structural integrity of the catalyst is maintained under reaction conditions. The XRD pattern of the spent CuO catalyst reveals diffraction peaks at  $2\theta = 43.4$ ,  $50.6$ , and  $74.1^\circ$ , attributed to the (111), (200), and (220) facets of pure copper (Cu) face-centered cubic structure (fcc), respectively. This shows that CuO is reduced to Cu during the oxidation of glucose to gluconic acid, suggesting that lattice oxygen in CuO is consumed in the oxidation reaction. However, the reoxidized catalyst (Figure 1d) reveals XRD peaks, similar to those of fresh CuO nanoleaves. This confirms

the regeneration of the catalyst and explains the excellent yields of gluconic acid, using the reoxidized catalyst.

The morphology and the structure of CuO nanoleaves were investigated using SEM and HRTEM. The images of the freshly prepared catalyst, the spent catalyst and the regenerated/reoxidized catalyst are shown in Figure 2. The leaf-like morphology of the fresh catalyst can be seen in Figure 2a,

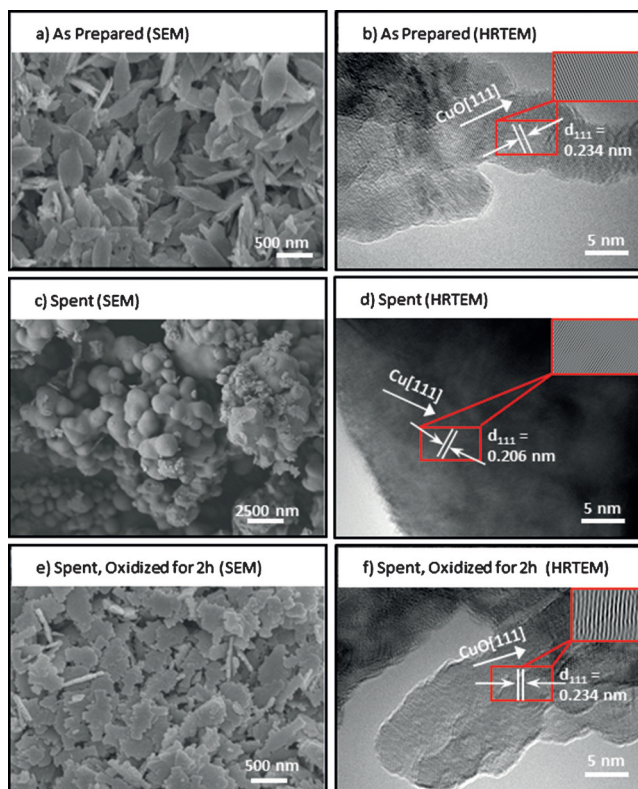


**Figure 2.** SEM and HRTEM images of (a,b) as-synthesized CuO nanoleaves, (c,d) CuO spent samples, and (e,f) CuO samples re-oxidized (regenerated) for 120 minutes in flowing oxygen of  $37 \text{ mL min}^{-1}$ .

with sizes less than a micron and thickness of about 30 nm. The nanoleaf is an assembly of 1D nanowires, in agreement with the proposed formation mechanism of 2D CuO by transformation and assembly of 1D Cu(OH)<sub>2</sub>.<sup>[10]</sup> The spent catalyst, upon removal of oxygen from the CuO lattice and after being reduced to Cu, however, acquires sphere-like morphology<sup>[11]</sup> (Figure 2c). After post-treating the spent CuO residues in oxygen flow for 120 minutes, almost complete transformation of sphere-like Cu particles back to leaf-like CuO morphology is observed (Figure 2e). BET surface area of the as-synthesized CuO was found to be  $23 \text{ m}^2 \text{ g}^{-1}$ , whereas the sphere-like spent catalyst had a surface area of  $4 \text{ m}^2 \text{ g}^{-1}$ , comparable to the surface area ( $5.64 \text{ m}^2 \text{ g}^{-1}$ ) of the sphere-like CuO reported earlier.<sup>[12]</sup> To better understand the effect of the nanoleaf morphology on the reaction, CuO nanocubes were also synthesized and characterized (Figure S6 in the Supporting Information). The XRD pattern of nanocubes is very similar to that of nanoleaves and their BET surface area is only  $4.07 \text{ m}^2 \text{ g}^{-1}$ . When tested for the reaction, nanocubes

resulted in 94.2 % conversion and 52.8 % gluconic acid yield. These results suggest that the higher surface-to-volume ratio of nanoleaves results in a higher active Cu(111) surface area (as explained later), and thus, higher yield of gluconic acid.

The HRTEM images of fresh, spent and regenerated CuO samples are shown in Figure 2b, 2d, and 2f, respectively. The lattice fringe of the CuO(111) fresh sample is regular, with a distance of 0.234 nm, and that of the spent catalyst is 0.206 nm, in agreement with existing literature.<sup>[13,14]</sup>

The regenerated CuO samples show a lattice fringe of 0.234 nm, similar to that of the fresh CuO sample. These results are in perfect agreement with our XRD and SEM analysis, suggesting the reduction of CuO to Cu during the glucose to gluconic acid reaction and its regeneration upon oxidation. CuO catalyzed glucose to gluconic acid oxidation reaction was also performed in O<sup>18</sup>-labeled water (H<sub>2</sub>O<sup>18</sup>), with the reactor being purged by nitrogen several times to ensure complete removal of any oxygen in the reactor. Analysis of reaction products using mass spectrometry did not reveal any O<sup>18</sup> in gluconic acid, further suggesting CuO as the source of oxygen for the reaction. Details of isotope studies are provided in section 6 of the Supporting Information.

To confirm the insertion of surface lattice oxygen of CuO into glucose, to reveal the underlying reaction mechanism and to investigate the role of lattice oxygen in enhancing the catalytic activity of CuO, we performed density functional theory (DFT) calculations. Computations were performed using the ab initio total-energy and molecular-dynamics program VASP (Vienna ab-initio simulation program)<sup>[15]</sup> and details are provided in section 2 of the Supporting Information. Simulations were performed on CuO(111) and Cu(111) surfaces to comprehensively evaluate the catalytic conversion of glucose to gluconic acid on the fresh/regenerated catalyst and on the spent catalyst (with and without chemisorbed oxygen), respectively. There are two different Cu sites on a CuO(111) surface; three coordinated Cu referred to as Cu<sub>3</sub> and four coordinated Cu referred to as Cu<sub>4</sub>. Similarly, there are O<sub>3</sub> and O<sub>4</sub> oxygen sites (refer to Figure S1 in the Supporting Information for details). The most stable structure (adsorption energy of 91 kJ mol<sup>-1</sup>) of the adsorbed glucose molecule on CuO(111) surface consists of the carbonyl carbon atom attached to the O<sub>3</sub> site and the carbonyl oxygen attached to two Cu<sub>3</sub> sites (compare Figure 3). Upon glucose adsorption, the surface lattice O<sub>3</sub> atom is pushed 0.33 Å above the original position. All the possible adsorption conformations are shown in Figure S7 of the Supporting Information.

The mechanism of glucose oxidation to gluconic acid involves the dissociation of the formyl C–H bond, formation of chemisorbed gluconate, hydrogenation of gluconate, and the desorption of gluconic acid. The reaction energy profile and the structures of transition states and intermediates for the oxidation of glucose to gluconic acid on CuO(111) surface are shown in Figure 3. In agreement with the experimental data, suggesting the incorporation of the lattice oxygen into glucose, the energy profile computed using DFT further corroborates the viability of the extraction of surface lattice oxygen from the CuO catalyst. The C–H bond is activated by two adjacent surface O<sub>3</sub> sites and the activation barrier for C–

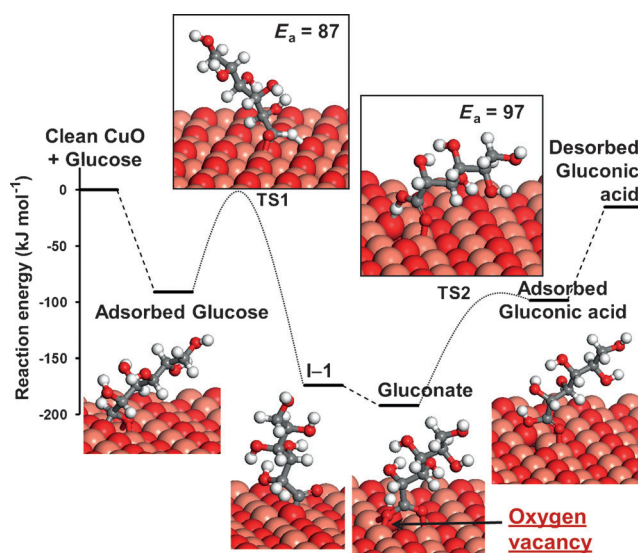


**Figure 3.** Energy profile for the oxidation of glucose to gluconic acid on CuO(111) surface. Reaction intermediates and transition states are shown. Activation energy barriers ( $E_a$ ) shown with the transition-state structures are in kJ mol<sup>-1</sup>. Copper color balls represent Cu atoms, red color balls represent O atoms, gray color balls represent C atoms, and white color balls represent H atoms.

H dissociation is only 87 kJ mol<sup>-1</sup>. After the C–H dissociation, the surface lattice oxygen atom that binds with the carbonyl carbon gets further pushed 0.11 Å higher from the surface. After C–H dissociation, formation of gluconate is downhill by 18 kJ mol<sup>-1</sup>. The strong binding of gluconate to the surface, by the bidentate configuration, could be the driving force to push the lattice oxygen out from the surface and generate the oxygen vacancy on the surface (Figure 3). This is similar to the generation of an oxygen vacancy on the CuO(111) surface, driven by H<sub>2</sub>O formation from adsorbed H and lattice oxygen.<sup>[16]</sup> In the structure of chemisorbed gluconate, the surface oxygen has completely come out from the lattice of CuO. Gluconate gets converted to adsorbed gluconic acid, with an activation barrier for the hydrogenation of 97 kJ mol<sup>-1</sup>. The transfer of H from the adjacent surface O<sub>3</sub> atom to the gluconate is endothermic by 92 kJ mol<sup>-1</sup>. Finally, the energy costs to desorb gluconic acid from the surface is 83 kJ mol<sup>-1</sup>. The activation of formyl C–H bond and the hydrogenation of adsorbed gluconate by the water-mediated hydrogen-shuttling pathway<sup>[17]</sup> were also evaluated by DFT calculations and by experiments, using deuterated water as the reaction medium (details provided in section 10 of the Supporting Information). Based on the results, it is suggested that the incorporation of water into the reaction mechanism is unlikely and the most preferred pathway is the one shown in Figure 3.

The complete mechanism of glucose oxidation to gluconic acid on Cu(111) is shown in Figure S9 of the Supporting Information. The adsorption energy of glucose on Cu(111) is only 21 kJ mol<sup>-1</sup> (as compared to 91 kJ mol<sup>-1</sup> on CuO). Because of the weaker binding of glucose on the Cu(111) surface, the activation energy barrier for C–H dissociation is increased to 141 kJ mol<sup>-1</sup> (TS1, Figure 4a). Compared to the



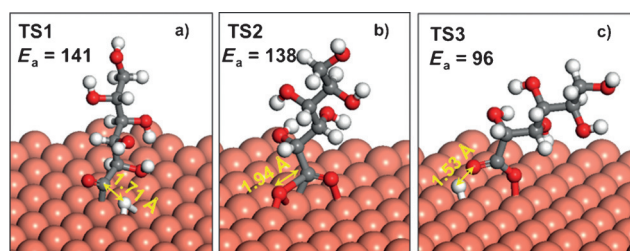


**Figure 4.** Transition states and activation energy ( $E_a$ ) barriers (in  $\text{kJ mol}^{-1}$ ) for the oxidation of glucose on Cu(111) surface. Glucose is adsorbed on the metal surface and the chemisorbed oxygen on the surface oxidizes it. The atom coloring scheme is the same as in Figure 3.

C–H dissociation on CuO(111), assisted by surface lattice oxygen atoms, the C–H scission on the Cu(111) surface has a much higher activation barrier. This explains the lower selectivity towards gluconic acid on the spent Cu catalyst. In the absence of lattice oxygen, molecular oxygen needs to be activated on the Cu(111) surface to oxidize the dehydrogenated glucose to form gluconate. The structure TS2 (Figure 4b) is the transition state for the combination of the chemisorbed oxygen and the dehydrogenated glucose to form gluconate. Hydrogenation of gluconate to adsorbed gluconic acid has an activation barrier of  $96 \text{ kJ mol}^{-1}$  (Figure 4c), in excellent agreement with literature.<sup>[18]</sup>

The activation barrier for  $\text{O}_2$  dissociation on Cu(111) is only  $28 \text{ kJ mol}^{-1}$ , consistent with the results of Mavrikakis.<sup>[19]</sup> This low barrier can facilitate the formation of chemisorbed oxygen on Cu(111) surface from the dissolved oxygen in water and it could possibly be a promising oxidant to oxidize glucose. However, the  $\text{O}_2$  dissociation reaction is extremely exothermic ( $-213 \text{ kJ mol}^{-1}$ ), and hence because of the strong Cu–O bond between the chemisorbed oxygen and the Cu(111) surface on the hollow fcc site,<sup>[19]</sup> the recombination of this oxygen with the dehydrogenated glucose could be challenging. This is consistent with our calculations, since the activation energy barrier for gluconate formation is as high as  $138 \text{ kJ mol}^{-1}$ . Additionally, the computed activation barrier for  $\text{H}_2\text{O}$  splitting on Cu(111) is  $132 \text{ kJ mol}^{-1}$ , in agreement with the barrier reported by the research groups of Li<sup>[20]</sup> and Mavrikakis.<sup>[21]</sup> This high activation barrier possibly hinders the formation of surface hydroxy groups to oxidize glucose. This further corroborates that water is not involved in the oxidation reaction.

The key steps in the oxidation of glucose to gluconic acid are the dissociation of the formyl C–H bond in glucose and the formation of chemisorbed gluconate. In the case of CuO(111), surface lattice oxygen atoms assist in the C–H dissociation and bring down the activation energy barrier to  $87 \text{ kJ mol}^{-1}$  (from  $141 \text{ kJ mol}^{-1}$  on Cu(111)). Besides, the formation of gluconate on CuO is easy because of the consumption of the surface lattice oxygen as oxidant; whereas the combination of chemisorbed oxygen with dehydrogenated glucose on Cu(111) is difficult. These results explain why CuO is a superior catalyst than Cu for the reaction. The lower activity of Cu(111) towards the oxidation of glucose to gluconic acid also explains the significant drop in gluconic

acid selectivity when CuO nanoleaves are reduced to Cu nanospheres.

To characterize the ability of surface-adsorbed oxygen activating the formyl C–H bond, two different scenarios were tested; one with glucose adsorbed on a single chemisorbed oxygen atom on Cu(111), where the carbonyl carbon is coordinated with the oxygen; and the other where glucose is adsorbed with the carbonyl carbon and the formyl hydrogen on two chemisorbed (dissociated) oxygen atoms, which are in close proximity to each other. The most preferred reaction pathways are reported here, while other competitive pathways were also considered and evaluated and details are provided in section 10 of the Supporting Information. The adsorption of glucose by chemisorbed oxygen is energetically more favorable than that on pure Cu ( $\Delta E_{\text{ads}}$  on pure Cu is  $21 \text{ kJ mol}^{-1}$ ). The adsorption energy increases from  $38$  to  $62 \text{ kJ mol}^{-1}$  when glucose is coordinated by two chemisorbed oxygen atoms (compare Figure 5). The activation energy barrier for C–H dissociation systematically decreases with

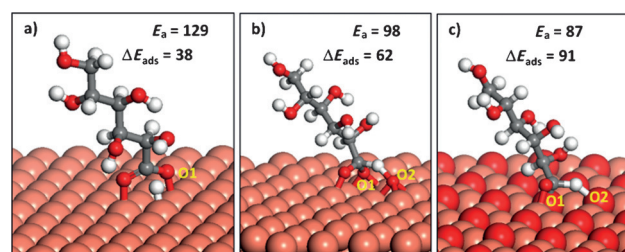


**Figure 5.** Transition states of the C–H bond dissociation on a) a single chemisorbed oxygen atom on Cu(111), b) cooperatively by two neighboring chemisorbed oxygen atoms on Cu(111), and c) by the surface lattice oxygen atoms in CuO(111). Oxygen atoms involved in the process are labelled. Activation energy barriers ( $E_a$ ) and adsorption energies ( $\Delta E_{\text{ads}}$ ) are in  $\text{kJ mol}^{-1}$ . The atom coloring scheme is same as in Figure 3.

increase in the adsorption energy of glucose. The barrier is highest for pure Cu(111) ( $141 \text{ kJ mol}^{-1}$ ), followed by  $129 \text{ kJ mol}^{-1}$  for glucose adsorbed on a single chemisorbed oxygen on Cu(111),  $98 \text{ kJ mol}^{-1}$  for glucose adsorbed on two adjacent chemisorbed oxygen atoms on Cu(111) and  $87 \text{ kJ mol}^{-1}$  for CuO(111). The decrease in the C–H bond activation barrier is consistent with the findings of Norskov and co-workers.<sup>[3c]</sup> When glucose adsorbs on the oxygen species on (or within) the surface, the C–H dissociation directly forms gluconate, and hence the mechanism is slightly different from that on pure Cu(111). However, the possibility of having two chemisorbed oxygen atoms on a Cu surface at such a close proximity that both carbon and hydrogen atoms of the formyl group can be coordinated, as shown in Figure 5b, is remote. Literature on oxygen–copper systems suggests that chemisorbed oxygen could only be present at extremely low coverage (metastable) and that thin surface oxide structures are more stable than chemisorbed oxygen. Additionally, there is a strong repulsion between partially negatively charged oxygens.<sup>[16,22]</sup> This is in excellent agreement with our experimental data, which shows excellent

glucose to gluconic acid activity for CuO only and the ease of regeneration of CuO nanoleaves on oxidation.

In summary, the oxidation of glucose to gluconic acid on CuO proceeds by the adsorption of glucose on surface lattice oxygen atoms of CuO(111), dissociation of the formyl C–H bond in glucose, the formation of gluconate, and the hydrogenation of gluconate to gluconic acid. The reduced CuO catalyst, in the form of nanoleaves, can be regenerated effectively upon oxidation. Implementing a combined experimental and theoretical approach, we reveal that the surface lattice oxygen in CuO(111) activates the formyl C–H bond in glucose by the virtue of strong adsorption of glucose and it further moves out of the lattice to get inserted into the glucose molecule for its oxidation to gluconic acid. Energy barriers for C–H dissociation and gluconate formation on pure Cu are significantly higher. The presence of chemisorbed oxygen atoms on Cu increases the adsorption energy of glucose and also activates the C–H bond (to a lesser extent though than surface lattice oxygen); however, chemisorbed oxygen atoms on Cu may not exist under experimental conditions. The CuO nanoleaves also give excellent yields of gluconic acid, with cellobiose and cellulose as starting materials.

**Keywords:** biomass · catalysis · C–H bond activation · lattice oxygen · sustainable chemistry

**How to cite:** *Angew. Chem. Int. Ed.* **2015**, *54*, 8928–8933  
*Angew. Chem.* **2015**, *127*, 9056–9061

- [1] a) A. Clark, *Ind. Eng. Chem.* **1953**, *45*, 1476–1480; b) R. Coquet, K. L. Howard, D. J. Willock, *Metal Oxide Catalysis*, Wiley-VCH, Weinheim, **2009**, pp. 323–389; c) M. B. Gawande, R. K. Pandey, R. V. Jayaram, *Catal. Sci. Technol.* **2012**, *2*, 1113–1125; d) S. Royer, D. Duprez, *ChemCatChem* **2011**, *3*, 24–65; e) H. Tsuji, H. Hattori, *ChemPhysChem* **2004**, *5*, 733–736.
- [2] a) G. I. Panov, A. K. Uriarte, M. A. Rodkin, V. I. Sobolev, *Catal. Today* **1998**, *41*, 365–385; b) T. V. Andrushkevich, *Catal. Rev.* **1993**, *35*, 213–259; c) T. Ono, T. Nakajo, T. Hironaka, *J. Chem. Soc. Faraday Trans.* **1990**, *86*, 4077–4081; d) M. R. Benjaram, *Metal Oxides*, CRC Press, Boca Raton, FL, **2005**, pp. 215–246; e) M. A. Peña, R. M. Navarro, J. L. G. Fierro, *Metal Oxides*, CRC Press, Boca Raton, FL, **2005**, pp. 463–490; f) U. Menon, V. V. Galvita, G. B. Marin, *J. Catal.* **2011**, *283*, 1–9; g) B. Grzybowska-Świerkosz, *Top. Catal.* **2000**, *11–12*, 23–42; h) S. Minicò, S. Scirè, C. Crisafulli, R. Maggiore, S. Galvagno, *Appl. Catal. B* **2000**, *28*, 245–251; i) S. Scirè, S. Minicò, C. Crisafulli, S. Galvagno, *Catal. Commun.* **2001**, *2*, 229–232.
- [3] a) G. J. Hutchings, M. S. Scurrell, J. R. Woodhouse, *Appl. Catal.* **1988**, *38*, 157–165; b) M.-S. Liao, Q.-E. Zhang, *J. Mol. Catal. A* **1998**, *136*, 185–194; c) J. S. Yoo, T. S. Khan, F. Abild-Pedersen, J. K. Norskov, F. Studt, *Chem. Commun.* **2015**, *51*, 2621–2624.
- [4] H.-Y. Li, Y.-L. Guo, G.-Z. Lu, P. Hu, *J. Chem. Phys.* **2008**, *128*, 051101.
- [5] H. Tsuji, A. Okamura-Yoshida, T. Shishido, H. Hattori, *Langmuir* **2003**, *19*, 8793–8800.
- [6] a) B. Girisuta, L. P. B. M. Janssen, H. J. Heeres, *Chem. Eng. Res. Des.* **2006**, *84*, 339–349; b) S. Govindaswamy, L. M. Vane, *Bioresour. Technol.* **2010**, *101*, 1277–1284; c) S. Naik, V. V. Goud, P. K. Rout, A. K. Dalai, *Renewable Sustainable Energy Rev.* **2010**, *14*, 578–597; d) H. Zhao, J. E. Holladay, H. Brown, Z. C. Zhang, *Science* **2007**, *316*, 1597–1600.
- [7] F. Wang, Y. Wang, F. Jin, G. Yao, Z. Huo, X. Zeng, Z. Jing, *Ind. Eng. Chem. Res.* **2014**, *53*, 7939–7946.
- [8] a) S. A. Nolen, C. L. Liotta, C. A. Eckert, R. Glaser, *Green Chem.* **2003**, *5*, 663–669; b) C. Luo, S. Wang, H. Liu, *Angew. Chem. Int. Ed.* **2007**, *46*, 7636–7639; *Angew. Chem.* **2007**, *119*, 7780–7783.
- [9] Z. Kebin, W. Ruipu, X. Boqing, L. Yadong, *Nanotechnology* **2006**, *17*, 3939.
- [10] M. Xu, F. Wang, B. Ding, X. Song, J. Fang, *RSC Adv.* **2012**, *2*, 2240–2243.
- [11] J. Xu, R. Fan, J. Wang, M. Jia, X. Xiong, F. Wang, *Int. J. Mol. Sci.* **2014**, *15*, 6412–6422.
- [12] A. A. Farghali, M. Bahgat, A. Enaiet Allah, M. H. Khedr, *Beni-Suef University J. Basic Appl. Sci.* **2013**, *2*, 61–71.
- [13] F.-C. Duh, D.-S. Lee, Y.-W. Chen, *Mod. Res. Catal.* **2013**, *2*, 1.
- [14] S. Krishnan, A. S. M. A. Haseeb, M. Johan, *J. Nanopart. Res.* **2013**, *15*, 1–9.
- [15] a) G. Kresse, J. Hafner, *Phys. Rev. B* **1993**, *47*, 558–561; b) G. Kresse, J. Furthmüller, *Comput. Mater. Sci.* **1996**, *6*, 15–50.
- [16] Y. Maimaiti, M. Nolan, S. D. Elliott, *Phys. Chem. Chem. Phys.* **2014**, *16*, 3036–3046.
- [17] D. D. Hibbitts, B. T. Loveless, M. Neurock, E. Iglesia, *Angew. Chem. Int. Ed.* **2013**, *52*, 12273–12278; *Angew. Chem.* **2013**, *125*, 12499–12504.
- [18] R. Zhang, L. Song, H. Liu, B. Wang, *Appl. Catal. A* **2012**, *443*, 444–50–58.
- [19] Y. Xu, M. Mavrikakis, *Surf. Sci.* **2001**, *494*, 131–144.
- [20] K. Yao, S.-S. Wang, X.-K. Gu, H.-Y. Su, W.-X. Li, *Chin. J. Catal.* **2013**, *34*, 1705–1711.
- [21] A. A. Gokhale, J. A. Dumesic, M. Mavrikakis, *J. Am. Chem. Soc.* **2008**, *130*, 1402–1414.
- [22] a) A. Soon, M. Todorova, B. Delley, C. Stampfl, *Surf. Sci.* **2007**, *601*, 5809–5813; b) S. Catherine, S. Aloysius, P. Simone, S. Hongqing, Z. Hong, *J. Phys. Condens. Matter* **2008**, *20*, 184021; c) A. Soon, M. Todorova, B. Delley, C. Stampfl, *Phys. Rev. B* **2006**, *73*, 165424.

Received: April 29, 2015

Published online: June 26, 2015